

Mechanism-based sirtuin enzyme activation

Raj Chakrabarti*

Division of Fundamental ResearchPMC Advanced Technology, LLC. 1288 Route 73 South, Mt. Laurel, NJ 08054, USA Phone: (609) 216-4644 Email: raj@pmc-group.com

Submitted to Proceedings of the National Academy of Sciences of the United States of America

Sirtuin enzymes are NAD⁺-dependent protein deacylases that play a central role in the regulation of healthspan and lifespan in organisms ranging from yeast to mammals. There is intense interest in the activation of the seven mammalian sirtuins (SIRT1-7) in order to extend mammalian healthspan and lifespan. However, there is currently no understanding of how to design sirtuin-activating compounds beyond allosteric activators of SIRT1-catalyzed reactions that are limited to particular substrates. Moreover, across all families of enzymes, only a dozen or so distinct classes of non-natural small molecule activators have been characterized, with only four known modes of activation among them. None of these modes of activation are based on the unique catalytic reaction mechanisms of the target enzymes. Here, we report a general mode of sirtuin activation that is distinct from any of the known modes of enzyme activation. Based on the conserved mechanism of sirtuin-catalyzed deacylation reactions, we establish biophysical properties of small molecule modulators that can result in enzyme activation for any sirtuin and any substrate. Building upon this framework, we propose mechanism-based workflows for the design of new sirtuin-activating compounds.

Sirtuins | Sirtuin activators | Kinetic modelling

Introduction

Sirtuin (silent information regulator) enzymes, which catalyze NAD⁺-dependent protein post-translational modifications, have emerged as critical regulators of many cellular pathways. In particular, these enzymes protect against age-related diseases and serve as key mediators of longevity in evolutionarily distant organismic models [1]. Sirtuins are NAD⁺-dependent lysine deacylases, requiring the cofactor NAD⁺ to cleave acyl groups from lysine side chains of their substrate proteins, and producing nicotinamide (NAM) as a by-product. A thorough understanding of sirtuin chemistry is not only of fundamental importance, but also of considerable medicinal importance, since there is enormous current interest in the development of new mechanism-based sirtuin modulators [2, 3]. The mechanism of sirtuin-catalyzed, NAD⁺-dependent protein deacylation is depicted in Fig. 1 [4-6].

Recently, in order to extend mammalian healthspan and lifespan, intense interest has developed in the activation of the seven mammalian sirtuin enzymes (SIRT1-7) [7,8,9]. Prior work on sirtuin activation has relied exclusively on experimental screening, with an emphasis on allosteric activation of the SIRT1 enzyme. Indeed, small molecule allosteric activators of SIRT1 have been demonstrated to induce lifespan extension in model organisms such as mice [7, 8]. Allosteric activation is one of four known modes by which small molecules can activate enzymes [10]. Allosteric activators most commonly function by decreasing the dissociation constant for the substrate (the acylated protein dissociation constant $K_{d,Ac-B}$ in the case of sirtuins).

Nearly all known sirtuin activators allosterically target SIRT1 and bind outside of the active site to an allosteric domain in SIRT1 that is not shared by SIRT2-7 [9]. Moreover, allosteric activators only work with a limited set of SIRT1 substrates [11-13]. It is now known that other sirtuins -- including SIRT2, SIRT3 and SIRT6 -- and multiple protein substrates play significant roles in regulating mammalian longevity [14-16]. General strategies for the activation of any mammalian sirtuin (including activation of

SIRT1 for other substrates) are hence of central importance, but not understood [17]. In general, allosteric activation to decrease substrate K_d will not be an option for enzyme activation, rendering mechanism-based activation essential.

Foundations for the rational design of mechanism-based sirtuin activators have been lacking, partly due to the absence of a clear understanding of the kinetics of sirtuin-catalyzed deacylation. Several types of mechanism-based sirtuin inhibitors have been reported recently in the literature, including Ex-527 and Sir-Real2 [18, 19]. However, mechanism-based activation has proven far more elusive, due to the difficulty in screening for the balance of properties needed for a modulator to have the net effect of accelerating catalytic turnover. While there are many ways to inhibit an enzyme's mechanism, there are far fewer ways to activate it. These efforts have been hindered by the lack of a complete steady state kinetic model of sirtuin catalysis that accounts for the effects of both NAD⁺ and NAM on activity.

In the so-called "NAD⁺ world" picture of global metabolic regulation, the intracellular concentrations of the sirtuin cofactor NAD⁺, which can decrease with age, play a central role in regulating mammalian metabolism and health through sirtuin-dependent pathways [20]. Due to the comparatively high Michaelis constants for NAD⁺ (K_{m,NAD^+} 's) of mammalian sirtuins, their activities are sensitive to intracellular NAD⁺ levels [4, 20]. The systemic decrease in NAD⁺ levels that accompanies organismic aging downregulates sirtuin activity and has been identified as a central factor leading to various types of age-related health decline [21, 22, 23], whereas increases in NAD⁺ levels can upregulate sirtuin activity and as a result mitigate or even reverse several aspects of this decline [20, 24].

Significance

Compared to enzyme inhibitors, which constitute the vast majority of today's drugs, enzyme activators have considerable advantages. However, they are much more difficult to design, because enzymatic catalysis has been optimized over billions of years of evolution. Sirtuin-activating compounds (STACs) are enzyme activators that can extend mammalian healthspan and lifespan. Unfortunately, the only known mode of STAC action is limited to accelerating selected functions of a single mammalian sirtuin enzyme. Here, we report a wholly new mode of enzyme activation that exploits the common catalytic mechanism of all sirtuin enzymes, hence being applicable to any function of any sirtuin. This expands our understanding of enzyme activation, and lays the foundation for development of a new generation of drugs.

Reserved for Publication Footnotes

137
138
139
140
141
142
143
144
145
146
147
148
149
150
151
152
153
154
155
156
157
158
159
160
161
162
163
164
165
166
167
168
169
170
171
172
173
174
175
176
177
178
179
180
181
182
183
184
185
186
187
188
189
190
191
192
193
194
195
196
197
198
199
200
201
202
203
204

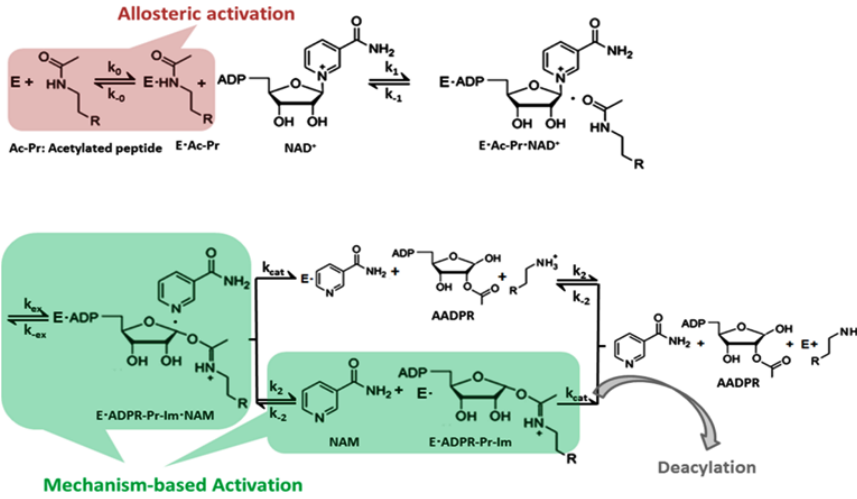


Fig. 1. Chemical mechanism of sirtuin-catalyzed deacylation and modes of sirtuin activation. Following sequential binding of acylated peptide substrate and NAD⁺ cofactor, the reaction proceeds in two consecutive stages: i) cleavage of the nicotinamide moiety of NAD⁺ (ADP-ribosyl transfer) through the nucleophilic attack of the acetyl-Lys side chain of the protein substrate to form a positively charged O-alkylimidate intermediate (depicted above), and ii) subsequent formation of deacylated peptide. For simplicity, all steps of stage ii as well as AADPR + Pr dissociation are depicted to occur together with rate limiting constant k_{cat} . **Red:** Allosteric activation increases the affinity of a limited set of peptide substrates for the SIRT1 enzyme only and requires an allosteric binding site. **Green:** Mechanism-based activation is a new mode of enzyme activation that relies on the conserved sirtuin reaction mechanism rather than an increase in the affinity of selected peptide substrates.

205
206
207
208
209
210
211
212
213
214
215
216
217
218
219
220
221
222
223
224
225
226
227
228
229
230
231
232
233
234
235
236
237
238
239
240
241
242
243
244
245
246
247
248
249
250
251
252
253
254
255
256
257
258
259
260
261
262
263
264
265
266
267
268
269
270
271
272

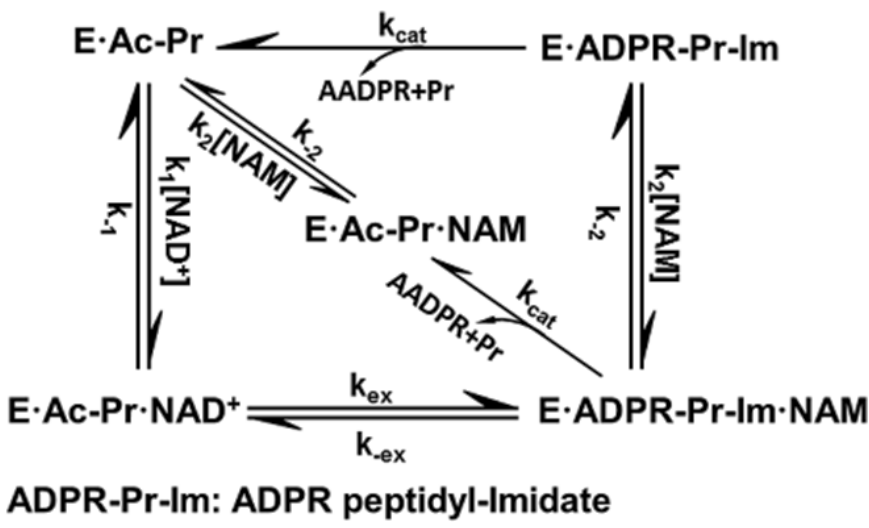


Fig. 2. General model for sirtuin-catalyzed deacylation in the presence of NAD⁺ and NAM. This model, based on the reaction mechanism depicted in Fig. 1, provides a minimal kinetic model that captures the essential features of sirtuin deacylation kinetics suitable for predicting the effects of mechanism-based modulators on sirtuin activity. In the presence of saturating Ac-Pr, E is rapidly converted into E·Ac-Pr and NAM binding to E can be neglected, resulting in a simplified reaction network with 5 species. Ac-Pr, acetylated peptide; ADPR, adenosine diphosphate ribose; AADPR, O-acetyl adenosine diphosphate ribose.

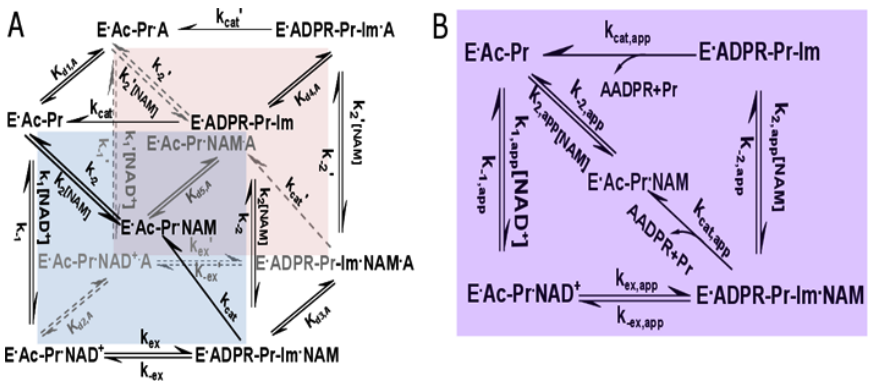


Fig. 3. General model for mechanism-based sirtuin enzyme activation. A) The front face of the cube (blue) depicts the salient steps of the sirtuin reaction network in the absence of bound modulator. The back face of the cube (red) depicts the reaction network in the presence of bound modulator (denoted by "A"). Each rate constant depicted on the front face has an associated modulated value on the back face, designated with a prime that is a consequence of modulator binding. B) The purple face is the apparent reaction network in the presence of a nonsaturating concentration of modulator.

As such, NAD⁺ supplementation has emerged as a promising alternative to allosteric activation of sirtuins [24]. Unlike

allosteric activators like resveratrol, which are SIRT1-specific and have not been successfully applied to other sirtuins [10],

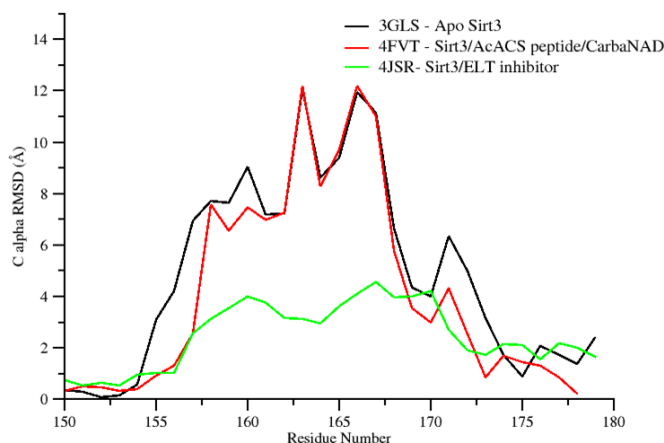


Fig. 4. Sirt3 cofactor binding loop region RMSD. Sirt3 proteins and their per-residue RMSD values for the cofactor binding loop region computed over all atoms with reference to crystal structure of a Sirt3 intermediate complex (4BVG). Residues (155-178) correspond to the co-factor binding loop region and residues (162-170) form a short alpha helix when bound to co-factors.

NAD⁺ supplementation can activate most mammalian sirtuins in a substrate-independent fashion. Moreover, allosteric activators cannot fully compensate for the reduction in sirtuin activity that occurs through NAD⁺ decline during aging. On the other hand, the effects of NAD⁺ supplementation are not specific to sirtuins and prohibitively high concentrations of NAD⁺, along with associated undesirable side effects, may be required to elicit the increases in sirtuin activity required to combat age-related diseases.

A preferred general strategy for activation of sirtuins (Fig. 1) would be to increase their sensitivity to NAD⁺ through a reduction of K_{m,NAD^+} . K_{m,NAD^+} reduction would have a similar activating effect to NAD⁺ supplementation, but would be selective for sirtuins and could potentially even provide isoform specific sirtuin activation. Importantly, due to the sirtuin nicotinamide cleavage reaction that involves the NAD⁺ cofactor, modulation of K_{m,NAD^+} may in principle be achievable by means other than altering the binding affinity of NAD⁺. Unlike allosteric activation that reduces $K_{d,Ac-Pr}$, this approach would be applicable to any sirtuin and any substrate.

In this paper, we present a general framework for activation of sirtuin enzymes that is distinct from any of the known modes of enzyme activation, based on the fundamental mechanism of the sirtuin deacylation reaction. We first introduce a steady-state model of sirtuin-catalyzed deacylation reactions in the presence of NAD⁺ cofactor and endogenous inhibitor NAM, and then establish quantitatively how K_{m,NAD^+} can be modified by small molecules, identifying the biophysical properties that small molecules must have to function as such mechanism-based activators. We propose workflows suitable for mechanism-based design of sirtuin activating compounds and present computational evidence supporting the existence of mechanism-based sirtuin activating compounds (MB-STACs) that operate according to the mechanisms presented.

Results

Steady-state sirtuin kinetic modeling

To a greater extent than inhibitor design, rational activator design requires the use of a mechanistic model in the workflow. In this section we develop a steady state model for sirtuin-catalyzed deacylation that is suitable for a) investigation of the mode of action of mechanism-based sirtuin modulators, including activators; b) design of mechanism-based sirtuin activating compounds. We first summarize the state of knowledge regarding the sirtuin-catalyzed deacylation mechanism.

The sirtuin catalytic cycle (Fig. 1) is believed to proceed in two consecutive stages [4]. The initial stage (ADP-ribosylation) involves the cleavage of the nicotinamide moiety of NAD⁺ and the nucleophilic attack of the acyl-Lys side chain of the protein substrate to form a positively charged O-alkylimidate intermediate [4, 24]. Nicotinamide-induced reversal of the intermediate (the so-called base exchange reaction) causes reformation of NAD⁺ and acyl-Lys protein. The energetics of this reversible reaction affects both the potency of NAM inhibition of sirtuins and the Michaelis constant for NAD⁺ (K_{m,NAD^+}). The second stage of sirtuin catalysis, which includes the rate-determining step, involves four successive steps that culminate in deacylation of the Lys side chain of the protein substrate and the formation of O-acetyl ADP ribose coproduct [4, 6, 25, 26].

A tractable steady state model suitable for the purpose of mechanism-based sirtuin activator design must account for the following important features:

- The calculated free energy of activation for nicotinamide cleavage (ADP-ribosylation of the acyl-Lys substrate) in the bacterial sirtuin enzyme Sir2Tm as computed through mixed quantum/molecular mechanics (QM/MM) methods is 15.7 kcal mol⁻¹ [27]. An experimental value of 16.4 kcal mol⁻¹ for the activation barrier in the yeast sirtuin homolog Hst2 was estimated from the reaction rate 6.7 s⁻¹ of nicotinamide formation [25]. The nicotinamide cleavage reaction is endothermic, with a computed ΔG of 4.98 kcal mol⁻¹ in Sir2Tm [27].

- The calculated free energy of activation for the rate limiting chemistry step (collapse of the bicyclic intermediate) from QM/MM simulations is 19.2 kcal mol⁻¹ for Sir2Tm [28], in good agreement with the experimental value of 18.6 kcal/mol⁻¹ estimated from the k_{cat} value of 0.170 ± 0.006 s⁻¹ [29] (0.2 ± 0.03 s⁻¹ for Hst2 [25]).

- The remaining steps in the catalytic cycle are significantly faster than the above steps. The other chemistry steps in stage 2 of the reaction are effectively irreversible [28], as is product release in the presence of saturating peptide concentrations.

We hence include in our kinetic model representations of all steps in stage 1 of the reaction, including the nicotinamide cleavage/base exchange and nicotinamide binding steps. However, for simplicity, we do not include in the present model a representation of each of the individual chemistry steps in stage 2 of the reaction or final product release, instead subsuming these steps under the smallest rate constant, which we call k_{cat} . Since all these steps are effectively irreversible, the full steady state model including these steps can be immediately derived from the basic model through simple modifications, to be described in a subsequent revision, that are not essential to the analysis of mechanism-based activation. The above observations motivate the kinetic model represented in Fig. 2 [30]. This Figure shows a general reaction scheme for sirtuin deacylation including base exchange inhibition.

The reaction mechanism of sirtuins precludes the use of rapid equilibrium methods for the derivation of even an approximate initial rate model; steady-state modeling is essential. The rate equations for the reaction network in Fig. 2 enable the derivation of steady-state conditions for the reaction. Solving the linear system of algebraic steady-state equations and mass balance constraints for the concentrations

$$[E_{Ac-Pr}], [E_{Ac-Pr} \cdot NAD^+], [E_{ADPR-Ac-Im} \cdot NAM], [E_{ADPR-Ac-Im}], [E_{NAM}]$$

in terms of the rate constants and $[NAD^+]$, $[NAM]$, which are assumed to be in significant excess and hence approximately equal to their initial concentrations $[NAD^+]_0$, $[NAM]_0$ respectively, we obtain expressions of the form (1):

409
410
411
412
413
414
415
416
417
418
419
420
421
422
423
424
425
426
427
428
429
430
431
432
433
434
435
436
437
438
439
440
441
442
443
444
445
446
447
448
449
450
451
452
453
454
455
456
457
458
459
460
461
462
463
464
465
466
467
468
469
470
471
472
473
474
475
476

477
478
479
480
481
482
483
484
485
486
487
488
489
490
491
492
493
494
495
496
497
498
499
500
501
502
503
504
505
506
507
508
509
510
511
512
513
514
515
516
517
518
519
520
521
522
523
524
525
526
527
528
529
530
531
532
533
534
535
536
537
538
539
540
541
542
543
544

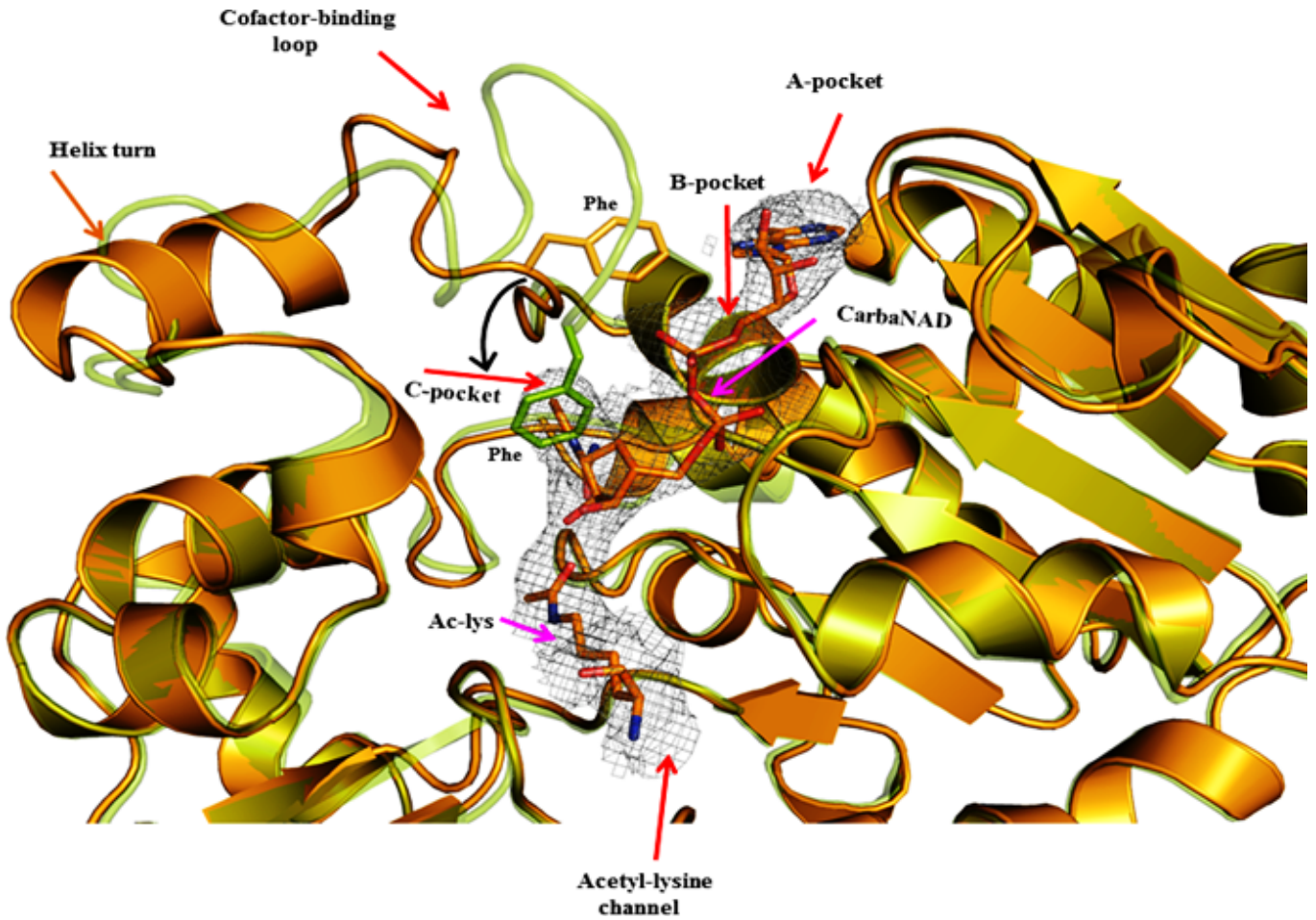


Fig. 5. : Structural superposition of Sirt3 structures. Superposition of Sirt3 native intermediate (4BVG - Green) and Sirt3 ternary complex (4FVT - Orange) showing differences in the conformation of the cofactor binding loop and the position of the Phe residue. Individual subsites are highlighted and the movement of Phe residue is indicated by black arrows. The substrates Carba-NAD and Ac-Lysine are rendered in stick representation.

$$[E \cdot Ac - Pr] / [E]_0 = c_{11} + c_{12} [NAM]$$

$$[E \cdot Ac - Pr \cdot NAD^+] / [E]_0 = c_{21} [NAD^+] + c_{22} [NAD^+] [NAM]$$

$$[E \cdot ADPR - Ac - Im \cdot NAM] / [E]_0 = c_{31} [NAD^+] + c_{32} [NAD^+] [NAM]$$

$$[E \cdot ADPR - Ac - Im] / [E]_0 = c_{41} [NAD^+]$$

$$[E \cdot Ac - Pr \cdot NAM] / [E]_0 = c_{51} [NAD^+] + c_{52} [NAM] + c_{53} [NAD^+] [NAM] + c_{54} [NAM]^2 \quad (1)$$

Where, the term c_{54} that is second order in $[NAM]$ will be omitted from the analysis below. Expressions for the c_{ij} 's are provided in the Appendix. The initial rate of deacylation can be then expressed

$$\frac{v}{v_{max}} = \frac{[NAD^+] \left(1 + \frac{[NAM]}{K_1} \right)}{K_{m,ADP} \left(1 + \frac{[NAM]}{K_2} \right) + [NAD^+] \left(1 + \frac{[NAM]}{K_3} \right)} \quad (2)$$

With

$$\begin{aligned} v_{max} &= \frac{k_{cat} * k_1 k_2 k_3 (k_2 + k_{cat})}{k_2 k_1 k_2 k_2 + k_{cat} (k_2 k_{cat} k_1 + k_2 k_2 k_1 + k_2 k_1 k_{cat} + k_2 k_1 k_2) + k_1 k_2 k_{cat}} [E]_0 \\ &\approx k_{cat} [E]_0 \\ K_{m,ADP} &= \frac{k_{cat} k_2 (k_{cat} k_{cat} + k_1 k_{cat} + k_{cat} k_2 + k_1 k_2 + k_{cat} k_1)}{k_2 k_1 k_2 k_2 + k_{cat} (k_2 k_{cat} k_1 + k_2 k_2 k_1 + k_2 k_1 k_{cat} + k_2 k_1 k_2) + k_1 k_2 k_{cat}} \\ &\approx k_{cat} \frac{k_{cat} k_2 + k_1 (k_2 + k_{cat})}{k_1 k_2 k_2} = k_{cat} \left(\frac{1}{k_1} + K_{m,ADP} \frac{k_2 + k_{cat}}{k_2 k_2} \right) \\ \frac{1}{K_1} &= \frac{k_1}{k_2 + k_{cat}} \approx \frac{1}{K_{d,NAM}} \quad (3a-e) \\ \frac{1}{K_2} &= \frac{1}{K_{m,ADP}} \frac{k_2 k_2 k_1 k_2 + k_{cat} (k_2 k_{cat} k_{cat} + k_1 k_2 k_{cat} + k_{cat} k_1 k_2 + 2k_2 k_2 k_1 + 2k_2 k_2 k_1)}{k_2 k_1 k_2 k_2 + k_{cat} (k_2 k_{cat} k_1 + k_2 k_2 k_1 + k_2 k_1 k_{cat} + k_2 k_1 k_2) + k_1 k_2 k_{cat}} \approx \frac{K_{d,NAD} K_{cat}}{K_{m,ADP} K_{d,NAM}} \\ \frac{1}{K_3} &\approx \frac{1}{\alpha K_1} = \frac{k_1 k_2 k_2 (k_{cat} + k_{cat}) + k_{cat} k_2 k_2 (k_2 + k_{cat})}{k_2 k_2 k_2 k_2 + k_{cat} (k_2 k_{cat} k_1 + k_2 k_2 k_1 + k_2 k_1 k_{cat} + k_2 k_1 k_2) + k_1 k_2 k_{cat}} \approx \frac{1 + K_{cat}}{K_{d,NAM}} \end{aligned}$$

Where $K_{ex} \equiv k_{-ex}/k_{ex}$ and the approximations refer to the case where

$$k_{cat} \ll k_j, j \neq cat$$

Equation (2) is typically represented graphically in terms of either double reciprocal plots at constant $[NAM]$ or Dixon plots at constant $[NAD^+]$. In the former case, the slope of the plot ($1/v$ vs $1/[NAD^+]$) at $[NAM]=0$ is $K_{m,ADP} / v_{max}$, for which the expression is:

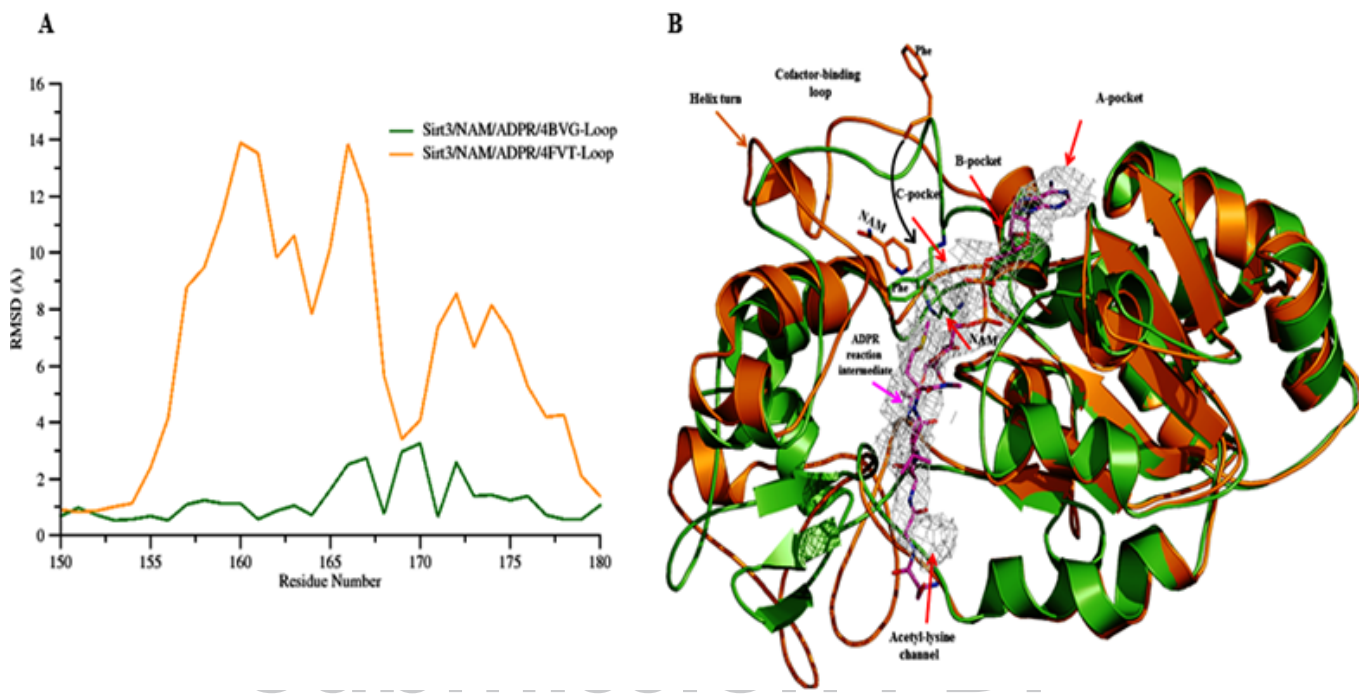


Fig. 6. Per-residue RMSD comparison for cofactor binding loop region. (A) Per-residue RMSD values for the cofactor binding loop region calculated using the MD averaged structure of Sirt3: ADPR: NAM complex modeled using the loop coordinates obtained from 4BVG (Green) and 4FVT (Orange). Crystal structure of a Sirt3 intermediate complex (4BVG) was used as the reference structure. Residues (162-170) form a short alpha helix when bound to co-factors. (B) Superposition of the time averaged MD structures of Sirt3/ADPR/NAM intermediate complex modelled based on the crystal structure of Sirt3 ternary complex (4FVT- orange) and another with the co-factor binding loop residues (155-178) being replaced from an native intermediate structure (4BVG-green). Differences in the conformations of the co-factor binding loop and the position of the Phe residue and NAM are highlighted. Individual subsites are highlighted; ADPR intermediate is rendered in sticks (carbons in Magenta) and NAM also shown in stick representation (Carbon atoms colored based on their respective protein cartoon color). A short helix is evident in Sirt3/ADPR/NAM intermediate complex modelled using 4FVT (Ternary complex), but not in the complex modelled using the co-factor binding loop replaced from the 4BVG (Native intermediate).

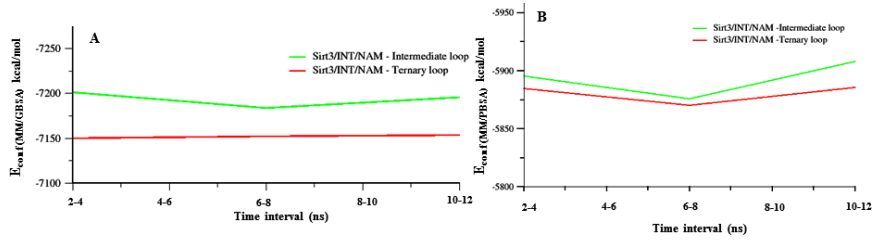


Fig. 7. Conformational energies of Sirt3-INT-NAM complexes. Conformational energies estimated using MM/PBSA and MM/GBSA method showing the energy gap for the Sirt3/INT/NAM complexes with different cofactor loop conformation. SIRT3/INT/NAM prepared from 4FVT with loop residues (res 155-178) replaced from 4FVT is shown in green and SIRT3/INT/NAM prepared from 4FVT with its native loop is shown in red. Panel A shows a plot of MM/GBSA conformational energy vs time and B shows plot of MM/PBSA vs times for the two different conformers.

Table 1. Conformation energy differences and binding energy difference for Sirt3 intermediate complex with different loop conformation calculated using calculated with the MM/PBSA and MM/GBSA method. Energy values are reported in kcal/mol.

Conformational energy difference of the Sirt3 intermediate complex			
Energy components for the complex	ΔG_A (SIRT3/INT/NAM prepared from 4FVT)	ΔG_B SIRT3/INT/NAM prepared from 4FVT with loop (res 155-178) replaced from 4BVG	$\Delta \Delta G_{(B \rightarrow A)}$ and $\Delta \Delta_{BE(B \rightarrow A)}$
$\langle E_{MM/GBSA} \rangle$	-7146.48 ± 3.55	-7201.58 ± 3.44	-55.10
$\langle E_{MM/PBSA} \rangle$	-5873.69 ± 3.87	-5901.23 ± 3.76	-27.54
$\Delta_{BE(MM/GBSA)} (\Delta E_{Complex} - \Delta E_{Receptor} - \Delta E_{Ligand})$	-20.33 ± 0.13	-22.50 ± 0.13	-2.17
$\Delta_{BE(MM/PBSA)} (\Delta E_{Complex} - \Delta E_{Receptor} - \Delta E_{Ligand})$	-3.96 ± 0.25	-7.73 ± 0.26	-3.77

* $\langle \rangle$ signifies ensemble average values computed from MD trajectories. The standard errors (\pm) for the values are also provided. $\langle E_{MM/GBSA} \rangle$ and $\langle E_{MM/PBSA} \rangle$ signifies the conformational energies of the Sirt3-INT-NAM complex. $\Delta_{BE(MM/GBSA)}$ and $\Delta_{BE(MM/PBSA)}$ signifies the binding energy of NAM for Sirt3. $\Delta \Delta G_{B \rightarrow A}$ signifies the conformational energy differences between two conformational states (B and A) which vary in the cofactor loop conformation. $\Delta \Delta_{BE(B \rightarrow A)}$ quantifies the relative binding energy difference of NAM for Sirt3 between two conformational loop conformations (B and A).

$$\frac{K_{m,NAD^+}}{v_{max}} \approx \frac{1}{[E]_0} \left(\frac{1}{k_1} + K_{d,NAD^+} \frac{k_{-2} + k_{-ex}}{k_{-2}k_{ex}} \right) \approx \frac{K_{m,NAD^+}}{k_{cat}[E]_0} \quad (4)$$

- Catalytic efficiency of sirtuins cannot be improved by increasing k_{cat} . Hence was not important to include rep of stage 2 of reaction in model

whereas for the Dixon plot, the expression for the slope at $1/[NAD^+] = 0$ is approximately [30]:

$$\frac{1}{K_3} \frac{1}{v_{max}} \approx \frac{1 + K_{ex}}{K_{d,NAM}} \frac{1}{k_{cat}[E]_0} \quad (5)$$

The steady state parameter α in equation (3e), which is a measure of the extent of competitive inhibition by the endogenous inhibitor NAM against the cofactor NAD⁺, can be expressed in terms of the ratio of K_{d,NAD^+} and K_{m,NAD^+} [29]:

$$\alpha = \frac{K_3}{K_2} \approx \frac{K_{d,NAD^+}}{K_{m,NAD^+}} \frac{K_{ex}}{1 + K_{ex}} \quad (6)$$

which, together with expression (3b) for K_{m,NAD^+} , demonstrates how the kinetics of inhibition of deacylation by NAM can reveal differences in NAD⁺ binding affinity and nicotinamide cleavage rates among sirtuins. The origins of different NAD⁺ binding affinities among sirtuins were studied structurally and computationally in [30]. Given that K_{ex} is generally $\gg 1$ for sirtuins, it is apparent from eqn (6) that the difference in magnitudes of K_{d,NAD^+} and K_{m,NAD^+} for sirtuins is captured by α . K_{m,NAD^+} , not K_{d,NAD^+} alone, determines the sensitivity of sirtuin activity to NAD⁺, and can vary across this family of enzymes. The initial rate model and the definition of α allow K_{d,NAD^+} to be estimated (under suitable approximations) by steady state deacylation experiments that vary [NAM] as well as [NAD⁺].

In addition to the approximation $k_{cat} \square k_j, j \neq cat$, several experimental observations can further simplify the form of the expressions (4) for the sirtuin steady state constants. First, we assume $k_{-2} \gg k_j, j \neq -2$ based on viscosity measurements that suggest NAM dissociates rapidly following cleavage [30]. Under this approximation, the expression for K_{m,NAD^+} becomes:

$$K_{m,NAD^+} \approx k_{cat} \left(\frac{1}{k_1} + \frac{K_{d,NAD^+}}{k_{ex}} \right) \quad (7)$$

The magnitudes of the on/off rates for NAD⁺ binding also affect the accuracy of approximations to equations (2,3). Such approximations will be studied in greater detail in a subsequent work.

As can be seen from eqn (3b), the kinetics of the nicotinamide cleavage reaction and the rate limiting step of deacylation both play essential roles in determining the value of K_{m,NAD^+} . Note that in rapid equilibrium models of enzyme kinetics, which are not applicable to sirtuins, $K_m \approx K_d$. The difference between K_{d,NAD^+} and K_{m,NAD^+} has important implications for mechanism-based activation of sirtuins by small molecules [30]. In particular, as we will show in this work, decrease of K_{m,NAD^+} independently of K_{d,NAD^+} can increase the activity of sirtuins at [NAM] = 0. The kinetic model above establishes foundations for how this can be done.

Mechanism-based sirtuin activation

Previous attempts to develop a general approach to sirtuin activation [31, 32] only considered competitive inhibitors of base exchange, which cannot activate in the absence of NAM. This is not actually a form of enzyme activation, but rather derepression

of inhibition. By contrast, here we present paradigms and design criteria for activation of sirtuins in either the absence or presence of NAM. Based on expression (3b) for K_{m,NAD^+} , it is in principle possible to activate sirtuins (not just SIRT1) for any substrate by alteration of rate constants in the reaction mechanism other than k_1, k_{-1} and k_{cat} , so as to reduce K_{m,NAD^+} -- not $K_{d,Ac-Pr}$ as with allosteric activators, which increase the peptide binding affinity of SIRT1 in a substrate-dependent fashion. We now explore how this may be achieved by augmenting the kinetic model to include putative mechanism-based activators (A) that can bind simultaneously with NAD⁺ and NAM. Fig. 3 depicts the reaction diagram for mechanism-based activation of sirtuins.

Note that only the top and front faces of this cube are relevant to the mechanism of action of the previously proposed competitive inhibitors of base exchange [31, 32].

At any [A] there exist apparent values of each of the rate constants in the sirtuin reaction mechanism. These are denoted by "app" in the Figure. There are also corresponding "app" values of the steady state, Michaelis, and dissociation constants in equation (3). Moreover, at saturating [A] of a known activator, the modulated equilibrium and dissociation constants (which do not depend on determination of steady state species concentrations) can be estimated with only deacylation experiments according to the theory presented above. The exchange equilibrium constant K_{ex}' and NAD⁺, NAM dissociation constants K_{d,NAD^+}' and $K_{d,NAM}'$ in the presence of A are related to their original values as follows:

$$K_{d,NAD^+}' = K_{d,NAD^+} \frac{K_{d2,A}}{K_{d1,A}}; K_{ex}' = K_{ex} \frac{K_{d3,A}}{K_{d2,A}}; K_{d,NAM}' = K_{d,NAM} \frac{K_{d3,A}}{K_{d4,A}} \quad (8)$$

where the $K_{d,i,A}$'s are the dissociation constants for A depicted in Fig. 3.

In order to predict the effect on K_{m,NAD^+}' of a modulator with specified relative binding affinities for the complexes in the sirtuin reaction mechanism, it is important to develop a model that is capable of quantifying, under suitable approximations, the effect of such a modulator on the apparent steady state parameters of the enzyme. Since the full steady state expression relating the original to the apparent rate constants has many terms containing products of additional side and back face rate constants, we use a rapid equilibrium segments approach to arrive at simple definitions of the apparent Michaelis constant and other steady state constants for the reaction in terms of the original expressions for these constants and the dissociation constants for binding of A to the various complexes in the sirtuin reaction mechanism. This provides a minimal model with the least number of additional parameters required to model sirtuin activation mechanisms. In our treatment, we will assume that rapid equilibrium applies on both the side faces and the back face. Under this approximation, at low [A] the expressions for the induced changes in each of the rate constant products appearing in the coefficients c_{ij} and c_{ij}' , $i'=i$ of equation (1) (see Appendix for expressions for these products) are the same and linear in [A]. For example, in the case of E_{Ac-Pr} , the steady state species concentrations become:

$$\begin{aligned} [E_{Ac-Pr}]/[E_{Ac-Pr}]_0 &\approx c_{11} + c_{12}[NAM] \\ [E_{Ac-Pr,A}]/[E_{Ac-Pr}]_0 &\approx \frac{[A]}{K_{d1,A}} (c_{11} + c_{12}[NAM]) \end{aligned} \quad (9)$$

The rapid equilibrium segments expressions for all species concentrations in equation (1) in the presence of A are provided in the Appendix.

Expressions for apparent values of all steady state parameters introduced in equation (3) (i.e., modulated versions of constants $v_{max}, K_{m,NAD^+}, K_1, K_2, K_3$) in the presence of a given [A] can now be derived. In the following, several types of approximations will be invoked:

817
818
819
820
821
822
823
824
825
826
827
828
829
830
831
832
833
834
835
836
837
838
839
840
841
842
843
844
845
846
847
848
849
850
851
852
853
854
855
856
857
858
859
860
861
862
863
864
865
866
867
868
869
870
871
872
873
874
875
876
877
878
879
880
881
882
883
884

i: rapid equilibrium segments approximation
 ii: $k_{cat}(1+K_{d,A}) \square k_j(1+K_{d',A}), j \neq cat, l = 1, \dots, 5$
 iii: $k_{-2}(1+K_{d1,A}) \square k_j(1+K_{d',A}), j \neq -2, l = 1, \dots, 5$ (rapid NAM dissociation)

$$\frac{v_{max,app}}{[E]_0} = \frac{k_{cat,app}(c_{31,app} + c_{41,app})}{c_{21,app} + c_{31,app} + c_{41,app} + c_{51,app}}$$

$$\frac{k_{cat}^2 c_{41} (1 + [A] / K_{d4,A})}{c_{41} (1 + [A] / K_{d4,A})} = k_{cat} \approx k_{cat,app}$$

$$K_{m,NAD^+,app} = \frac{c_{11,app}}{c_{21,app} + c_{31,app} + c_{41,app} + c_{51,app}}$$

$$\frac{c_{11} \left(1 + \frac{[A]}{K_{d1,A}} \right)}{c_{21} \left(1 + \frac{[A]}{K_{d2,A}} \right) + c_{31} \left(1 + \frac{[A]}{K_{d3,A}} \right) + c_{41} \left(1 + \frac{[A]}{K_{d4,A}} \right) + c_{51} \left(1 + \frac{[A]}{K_{d5,A}} \right)}$$

$$\approx k_{cat} \left(\frac{1}{k_1} + \frac{K_{d,NAD^+,app}}{k_{ex,app}} \right) \frac{1 + [A] / K_{d1,A}}{1 + [A] / K_{d1,A}} \approx k_{cat,app} \left(\frac{1}{k_1} + \frac{K_{d,NAD^+,app}}{k_{ex,app}} \right) \frac{1 + [A] / K_{d1,A}}{1 + [A] / K_{d1,A}}$$

Recall that α provides an estimate of the ratio of the dissociation and Michaelis constants for NAD^+ .

$$\alpha_{app} \approx \frac{c_{12} (1 + [A] / K_{d2,A}) + c_{52} (1 + [A] / K_{d5,A})}{c_{22} (1 + [A] / K_{d2,A}) + c_{32} (1 + [A] / K_{d3,A}) + c_{52} (1 + [A] / K_{d5,A})} \frac{1}{K_{m,NAD^+,app}}$$

$$\approx \frac{K_{d,NAD^+} K_{ex}}{K_{m,NAD^+} (1 + K_{ex})} \frac{(1 + [A] / K_{d4,A})}{(1 + [A] / K_{d2,A})} \approx \frac{K_{d,NAD^+,app} K_{ex,app}}{K_{m,NAD^+,app} (1 + K_{ex,app})}$$

$$\alpha_{app} K_{m,NAD^+,app} \approx \frac{K_{ex}}{1 + K_{ex}} \frac{(1 + [A] / K_{d1,A})}{(1 + [A] / K_{d2,A})} \approx \frac{K_{d,NAD^+,app} K_{ex,app}}{1 + K_{ex,app}}$$

The latter provides an estimate of $K_{d,NAD^+,app}$ if $K_{ex} \square 1$, as it is believed to be for most sirtuins.

Under approximation (ii), K_3 isolates nicotinamide cleavage / base exchange-specific effects.

$$\frac{1}{K_{3,app}} \approx \frac{c_{22} (1 + [A] / K_{d2,A}) + c_{32} (1 + [A] / K_{d3,A}) + c_{52} (1 + [A] / K_{d5,A})}{c_{21} (1 + [A] / K_{d2,A}) + c_{31} (1 + [A] / K_{d3,A}) + c_{41} (1 + [A] / K_{d4,A}) + c_{51} (1 + [A] / K_{d5,A})}$$

$$\approx \frac{1 + K_{ex}}{K_{d,NAMd}} \frac{(1 + [A] / K_{d2,A})}{(1 + [A] / K_{d4,A})} \approx \frac{1 + K_{ex,app}}{K_{d,NAMd,app}}$$

$$\frac{1}{K_{2,app}} = \frac{c_{12,app} + c_{52,app}}{c_{11,app}} \approx \frac{c_{12} (1 + [A] / K_{d1,A}) + c_{52} (1 + [A] / K_{d5,A})}{c_{11} (1 + [A] / K_{d1,A})}$$

885
886
887
888
889
890
891
892
893
894
895
896
897
898
899
900
901
902
903
904
905
906
907
908
909
910
911
912
913
914
915
916
917
918
919
920
921
922
923
924
925
926
927
928
929
930
931
932
933
934
935
936
937
938
939
940
941
942
943
944
945
946
947
948
949
950
951
952

$$\frac{c_{12} (1 + [A] / K_{d1,A})}{c_{11} (1 + [A] / K_{d1,A})} = \frac{K_{d,NAD^+} K_{ex}}{K_{m,NAD^+} K_{d,NAMd}} \approx \frac{K_{d,NAD^+,app} K_{ex,app}}{K_{m,NAD^+,app} K_{d,NAMd,app}} \quad (15)$$

Regarding the quality of the approximations in this case, note from (15) and (A1) that unlike any of the other steady-state parameters, the modulation $\frac{1}{K_{2,app}} - \frac{1}{K_2}$ induced by [A] is proportional to k_{cat} under the rapid equilibrium segments approximation (first approximation above). Hence, if one is interested in estimating the sign of this modulation, the small k_{cat} approximation (second approximation above) should not be applied. Also, under the rapid equilibrium segments approximation, $K_{2,app}$ is the only constant that relies on a ratio of two c_{ij} 's with $i' = i, j' \neq j$, and hence the ratio of the same factor in [A]. It is obvious that the apparent values of rate constant products in the numerator and denominator above cannot be precisely equal and hence $K_{2,app}$ will have to change slightly from K_2 .

$$\frac{1}{K_{1,app}} = \frac{c_{32,app}}{c_{31,app} + c_{42,app}}$$

$$\approx \frac{k_1 k_{ex} k_2 k_{-2} (1 + [A] / K_{d3,A})}{k_{cat} k_1 k_{ex} k_{-2} (1 + [A] / K_{d3,A}) + k_1 k_{ex} k_2 k_{-2} (1 + [A] / K_{d4,A})}$$

$$\approx \frac{1}{K_{d,NAMd}} \frac{1 + [A] / K_{d3,A}}{1 + [A] / K_{d4,A}} \quad (16)$$

Conditions for mechanism-based activation

We now consider thermodynamic conditions on the binding of a modulator A for mechanism-based sirtuin activation under the rapid equilibrium segments approximation, along with the expected changes in the steady state, equilibrium and dissociation constants in the sirtuin reaction mechanism.

First, according to equation (10), $v_{max} / [E]_0$ is roughly unchanged within this family of mechanisms as long as the $K_{d,A}$'s for [A] binding to the various represented complexes in the reaction mechanism satisfy condition (iii). Thus, enzyme activation is expected if $K_{m,NAD^+,app}$ can be decreased relative to K_{m,NAD^+} - i.e., if the sensitivity of sirtuins to NAD^+ can be increased. According to equation (11), $K_{m,NAD^+,app}$ will be smaller than K_{m,NAD^+} if $K_{d1,A} / K_{d4,A} \geq (K_{d1,A} / K_{d2,A}) (K_{d2,A} / K_{d3,A}) (K_{d3,A} / K_{d4,A}) > 1$. To identify mechanisms by which this can occur in terms of the steps in the sirtuin-catalyzed reaction, we consider in turn each of these three respective ratios of $K_{d,A}$'s (or equivalently, the $\Delta\Delta G^\ddagger$'s of the NAD^+ binding, exchange, and NAM binding reactions as implied by equation (8)) induced by A binding.

According to equation (13), $K_{d1,A} / K_{d2,A} < 1$ would imply that A binding increases the binding affinity of NAD^+ to the E.Ac-Pr complex. This is biophysically implausible for mechanism-based activation; when dissociation constants for substrates decrease upon small molecule binding, this typically occurs through an allosteric mechanism.

Comparison of the crystal structure of human Sirt3/AcS2 peptide /Carba NAD ternary complex (4FVT) with Sirt3 apo structure (3GLS) shows the cofactor binding loop adapts a close-to-ternary loop conformation (See Fig 4 and Supporting Information --). 3GLS (apo structure) has close-to-ternary loop conformation (See Fig 4 and Supporting Information)

This means that it will be difficult to preferentially stabilize the ternary complex relative to the apo complex using a modula-

953
954
955
956
957
958
959
960
961
962
963
964
965
966
967
968
969
970
971
972
973
974
975
976
977
978
979
980
981
982
983
984
985
986
987
988
989
990
991
992
993
994
995
996
997
998
999
1000
1001
1002
1003
1004
1005
1006
1007
1008
1009
1010
1011
1012
1013
1014
1015
1016
1017
1018
1019
1020

In particular, this renders K_{d,NAD+} reduction more challenging than other types of K_{m,NAD+} reduction.

Thus, we assume that for a mechanism-based activator, $K_{d1,A} \geq K_{d2,A}$. Then, in order to have $K_{m,NAD+}^{app} < K_{m,NAD+}^*$, we require $(K_{d2,A} / K_{d3,A})(K_{d3,A} / K_{d4,A}) > K_{d1,A} / K_{d2,A}$ or equivalently, according to (8), $(K_{d,NAM} / K_{ex})(K_{ex} / K_{d,NAM}) > K_{d,NAD+} / K_{d,NAD+}$. The decrease in $K_{m,NAD+}^*$ can hence be due to modulation of the exchange rate constants that induces a decrease in K_{ex} , an increase in $K_{d,NAM}$, or both. We assume $K_{d,NAM} \geq K_{d,NAM}^*$ ($K_{d3,A} \geq K_{d4,A}$) for reasons analogous to those for $K_{d,NAD+}^*$ (NAM being the nicotinamide moiety of NAD+). This corresponds to mixed noncompetitive inhibition [30] of base exchange.

As we have previously shown [30], the nicotinamide moiety of NAD+ engages in nearly identical interactions with the enzyme before and after bond cleavage. The salient difference is a conformational change in a conserved phenylalanine side chain (e.g., Phe33 in Sir2Tm, Phe157 in SIRT3) that destabilizes NAM binding after bond cleavage [33, 34].

Since NAM binding is already destabilized by the native protein conformation in this way, and since $\Delta\Delta G_{bind,NAD+}^*$ induced by the modulator will generally be greater in magnitude than $\Delta\Delta G_{bind,NAM}^*$ due to disruption of additional contacts between the ADPR moiety of NAD+ and the enzyme, $K_{d3,A}$ is likely to make the dominant contribution to $K_{d4,A}$.

Note that there is ample scope for modulation of ΔG_{ex} by the modulator due to the coupling of the endothermic nicotinamide cleavage / ADP ribosylation reaction (exothermic base exchange reaction) to a conformational change in the sirtuin cofactor binding loop. ΔG_{ex} for Sir2Tm has been calculated to be -4.98 kcal/mol [27]. (For comparison, $\Delta G_{bind,NAM}^*$ for Sir2Af2 was estimated to be -4.1 kcal/mol [31] and $\Delta G_{bind,NAM}^*$ for SIRT3 was estimated to be <= -3.2 kcal/mol [30].) Tighter binding of modulators to the intermediate (ADPR-Pr-Im) complex compared to ternary substrate (NAD+, peptide)-bound complex is possible due to the fact that this substantial conformational rearrangement of sirtuin loops occurs universally upon NAM cleavage [34]. The flexible loop in 4BVG (intermediate complex) has a significantly higher RMSD with respect to that in 4FVT (ternary complex) than does the flexible loop in 3GLS (apo-enzyme). Hence it is plausible that the intermediate complex can bind more tightly to the ligand than the substrate complex through such flexible loop interactions. Across all sirtuins studied, nicotinamide cleavage induces similar structural changes (for example, unwinding of a helical segment in the flexible cofactor binding loop [33, 34]; see Fig 5 and Supporting Information ---) and such changes might enable preferential stabilization of the E.ADPR-Pr-Im complex, in a manner similar to the stabilization of specific loop conformations by mechanism-based inhibitors [18].

Note that sirtuin ELT inhibitors [35], which are peptidomimetics that also extend into the C pocket (through a NAM-mimicking moiety), induce a 4BVG (ADPR-Pr-Im complex)-like loop conformation with a similar alpha turn and without the helix that is present in the ternary loop conformation (See fig 4).

This suggests that modulators (if they do not compete with substrates) can induce the desired loop conformational changes / stabilization of ADPR-Pr-Im-like loop conformations.

Taken together, these observations suggest that $K_{d2,A} / K_{d3,A} > K_{d1,A} / K_{d4,A}$ and that the value of $K_{ex} / K_{d,NAM}$ required for activation is likely to be achieved primarily by altering the free energy change of the nicotinamide cleavage reaction. However, our model accommodates the possibility of arbitrary combinations of $\Delta\Delta G_{ex}^*$ and $\Delta\Delta G_{bind,NAM}^*$ contributing to activation.

Computational studies of the loop conformational change have not previously been reported. The closest prior study comprised QM/MM simulations of stage 2 of catalysis (starting from intermediate complex) [28]. In the present study MD simulations have been carried out on SIRT3/INT/NAM complex prepared from 4FVT with and without loop replacement that is taken from residue 155-178 of 4BVG.

Time averaged MD structure obtained revealed loss of structural stability for Sirt3/INT/NAM complex modeled using the ternary loop conformation (See fig 6 B). In addition the conformational energy of the complex as calculated using the Amber all-atom force field in conjunction with implicit solvent also suggest the complex to be energetically less stable in relation to the complex structure modeled using an loop conformation from an intermediate sirt3 complex.

Thus, we find that the following thermodynamic conditions on the binding of A to the various complexes in the sirtuin reaction mechanism are physically plausible and conducive to mechanism-based activation:

$$\begin{aligned} K_{d1,A} \leq K_{d2,A} &\Leftrightarrow K_{d,NAD+} \geq K_{d,NAD+}^* & (17) \\ K_{d2,A} \gg K_{d3,A} &\Leftrightarrow K_{ex} \square K_{ex}^* \\ K_{d3,A} \geq K_{d4,A} &\Leftrightarrow K_{d,NAM} \geq K_{d,NAM}^* \end{aligned}$$

where the \gg sign signifies that $K_{d2,A} / K_{d3,A} > K_{d1,A} / K_{d4,A}$.

Finally, in our original model for sirtuin kinetics in Fig. 2, we assumed that both $K_{d,NAM}^*$'s— namely, those for dissociation of NAM from E.Ac-Pr.NAM and E.ADPR-Pr-Im.NAM — are roughly equal. We maintain this condition in the presence of A binding, which is reasonable given that A is assumed to not interact directly with the peptide or ADPR moiety, and since NAM binding does not rely on interactions with the flexible cofactor binding loop [26, 29]. Hence, we have:

$$\frac{[E.ADPR-Pr-Im][NAM]}{[E.ADPR-Pr-Im.NAM]} \approx \frac{[E.Ac-Pr][NAM]}{[E.Ac-Pr.NAM]} \Leftrightarrow K_{d5,A} \approx \frac{K_{d1,A}K_{d3,A}}{K_{d4,A}} \quad (18)$$

We now consider the effects of binding of a modulator A that satisfies the above requirements for activation on the remaining steady state constants.

- α_{app} : According to equation (12), the aforementioned requirement for activation that $K_{d2,A} / K_{d4,A} \geq K_{d1,A} / K_{d4,A}$ implies a significant increase in α by a factor that will generally exceed $K_{m,NAD+} / K_{m,NAD+}^{app}$.

- $K_{3,app}$: According to equation (14), in the presence of such a mechanism-based activator, K_3 is expected to increase by a factor similar to that for α under the rapid equilibrium segments approximation. This can occur due to an increase in $K_{d,NAM}$, decrease in K_{ex} , or both. Decrease in K_{ex} corresponds to hyperbolic (or partial) noncompetitive inhibition [30] of base exchange/activation of nicotinamide cleavage. With an additional increase in $K_{d,NAM}$, noncompetitive inhibition of base exchange becomes mixed non-competitive inhibition of base exchange. Additional information (e.g., from high [NAM] initial rate experiments, which permit estimation of $K_{d,NAM,app}$) is required to separate these possible causes.

- $K_{2,app}$: With conditions (17), equation (14) predicts a small increase in K_2 since $K_{d5,A} > K_{d1,A}$. K_2 increases to a smaller extent than K_3 .

- $K_{1,app}$: With conditions (17), equation (16) predicts an increase in K_1 .

A salient feature of this mechanism-based model for enzyme activation is that the intermediate reaction step is accelerated and

made more thermodynamically favorable at expense of destabilization of substrate binding. Instead of competition with respect to NAM for binding, then, selective stabilization of the reaction intermediate through preferential binding to structural features unique to the intermediate – in particular, an altered flexible loop conformation – may be capable of activating sirtuins. Binding energy estimates computed using MM/PBSA and MM/GBSA method also reveal the transition state (TS) intermediate to have preferential binding towards Sirt3 with an intermediate co-factor loop conformation over a ternary loop conformation (See Table 1). The conformational energies of the complex show that Sirt3/Int/NAM complex with an intermediate co-factor loop conformation to be energetically more stable. In order for this to be possible, the free energy gap ΔG between such protein conformations must be sufficiently large for K_{d3} , $A/K_{d2,A}$ to be far enough from unity to produce a substantive change in the energetics of the reaction. In that case, according to the steady state model, selective stabilization of a loop conformation similar to that in the intermediate complex can have the net result of activation.

-Destabilization of secondary structure by ternary loop conformation in INT complex depicted above: consistent with MM-GBSA results and suggests that there are destabilizing (unfavorable) interactions between INT and ternary loop

Returning to equation (11) for $K_{m,NAD^+_{app}}$ and substituting $(1+[A]/K_{d2,A})/(1+[A]/K_{d1,A}) \geq 1$, the rapid equilibrium assumptions applied to the present system imply that in order to activate the enzyme at $[NAM]=0$, A must increase k_1 ($k_{1,app} > k_1$), k_{ex} ($k_{ex,app} > k_{ex}$) or both. The rapid equilibrium segments model is not able to distinguish between these scenarios, but given that A is prone to increase $K_{d,NAD^+_{app}}$, assuming that it also increases k_1 is physically implausible. An increase in k_{ex} implies acceleration of the rate of nicotinamide cleavage. In the rapid equilibrium segments framework, this occurs through preferential stabilization of the E.ADPR-Pr-Im complex.

We discuss below the biophysical underpinnings whereby an increase in a forward rate constant could be achieved through preferential stabilization of the intermediate complex.

Potential means of increasing k_{ex}

From the standpoint of chemical mechanisms of activation, the theory presented raises the important question of how the nicotinamide cleavage rate k_{ex} of sirtuins can be accelerated by a ligand that binds to the various complexes in the deacylation reaction with the specified relative affinities, as predicted by equation (11). It is important to note in this regard that the nicotinamide cleavage reaction in sirtuins is generally believed to be endothermic, which enables effective NAM inhibition of the reaction [26, 36]. Unlike exothermic reactions, stabilization of products or destabilization of reactants in endothermic reactions can decrease the activation barrier for the forward reaction, due to the fact that the transition state resembles the products more than the reactants. The energetics of this reaction, including the role of protein conformational changes, is being studied computationally in our group for mammalian sirtuins.

Discussion

We have presented a model for activation of sirtuin enzymes suitable for the design and characterization of mechanism-based sirtuin activating compounds (MB-STACs) that can in principle activate any of the mammalian sirtuins SIRT1-7, unlike previously proposed strategies for sirtuin activation. Also, the activation model presented herein should be applicable to any substrate, unlike previously reported allosteric activation of SIRT1 that was found to accelerate deacylation for only a small fraction of over 6000 physiologically relevant peptide substrates studied, due to the need for “substrate-assistance” in the allosteric mechanism [13]. Moreover, this framework comprises a new mode of enzyme

activation that is distinct from any of the four modes of activation previously known across all families of enzymes.

Using this modeling framework, we have shown how modulation of K_{m,NAD^+} independently of K_{d,NAD^+} can increase the activity of sirtuins at $[NAM]=0$ in a manner that mimics the effects of NAD^+ supplementation [36] but in a selective fashion. This activation also applies at nonzero $[NAM]$, decreasing the sensitivity of the sirtuin to physiological NAM inhibition in addition to increasing its sensitivity to physiological NAD^+ . Such mechanism-based sirtuin activation has advantages over a) allosteric activation, which is only possible for SIRT1, is substrate-dependent, and cannot fully compensate for the reduction in NAD^+ levels that is responsible for many aspects of health decline during organismic aging [11, 12, 37]; b) activation of the NAD^+ biosynthetic enzyme Nampt [38], which regenerates NAD^+ from NAM and hence has nonselective effects on all enzymes that use an NAD^+ cofactor; and c) inhibition of NAD^+ -dependent PARP enzymes, which consume NAD^+ but are required to repair DNA damage [23]. Moreover, it has the potential to enable isoform-specific sirtuin enzyme activation.

The rapid equilibrium segments approximation (Appendix, equation A3) was applied in order to illustrate how a ligand that binds outside the NAD^+ binding site can in principle increase sirtuin activity through only modulation of the relative free energies of the various species in the reaction mechanism. More detailed analysis of the mechanism of action of MB-STACs can be achieved by complete kinetic characterization in presence/absence of the activator (e.g., by coupling base exchange with deacylation experiments). Such analyses will shed light on whether mechanism-based sirtuin activation exploits the free energy profile of the sirtuin nicotinamide cleavage and base exchange reactions – and if so, how. Note that, as discussed, the nicotinamide cleavage step is reversible and the DHP activator both decreases the NAM sensitivity of the sirtuin and activates at $[NAM]=0$. Besides DHPs, it is worthwhile to apply the mechanism identification methodology presented herein to any STACs that may be found to activate either SIRT2-7 or SIRT1-catalyzed reactions on substrates other than those of the limited type identified in [11-13] to which traditional STACs are restricted. The opportunities for mechanism-based activation of mammalian sirtuins will depend on their particular values of K_{m,NAD^+} and the underlying values of the associated rate constants. Importantly, a sirtuin need not be highly sensitive to base exchange inhibition in order to be susceptible to mechanism-based activation.

Structurally, binding outside of the NAD^+ binding site (the so-called A and C pockets [26, 39]) appears to be essential for mechanism-based activation. We are currently exploring prospective binding sites for MB-STACs. Moreover, rational design will require analysis of the relative free energies of complexes depicted in Fig. 3. We have recently initiated computational studies [30] that assess such free energy differences for some of the front face (apo) complexes in this Figure, and further studies are in progress.

The enzyme activation theory presented herein motivates experimental workflows for the hit identification, hit-to-lead evolution, and lead optimization of mechanism-based activators. In particular, the theory enables the identification and evolution of important hits that may be inhibitors, not activators, by decomposing the observed kinetic effects of a modulator into components and identifying those molecules that display favorable values of a subset of these components as hits even if the net effect on catalytic turnover is inhibition. Compared to standard library screening for hit identification and hit-to-lead evolution, this approach allows application of multiobjective optimization techniques (through iterative mutations to functional groups) to sirtuin activator design. Such workflows would be fundamentally different from traditional drug discovery workflows and would

bear more similarity to the directed evolution of enzymes. The theory presented also establishes foundations for the rational design of sirtuin-activating compounds, enabling the application of state-of-the-art computational methods to activator design in a manner analogous to computational enzyme design [40]. Finally, it raises the important question as to whether other enzyme families may also be activatable through such a mechanism-based mode of action -- and if so, which families.

The enzyme activation theory presented herein raises the question as to whether other enzyme families may also be activat-

able through mechanism-based design-- and if so, which families. Certainly, its application to other NAD⁺-dependent enzymes, such as poly- and mono ADP ribosyl transferases, should be considered. In principle, mechanism-based enzyme activation could be used to selectively activate particular ADP ribosyl transferases, increasing their sensitivity to NAD⁺ as its levels decline with age. The potential diversity of the newly reported mode of mechanism-based enzyme activation far exceeds that of allosteric activation for such families of enzymes.

Computational Methodology

1. Kaeberlein M, McVey M, & Guarente L (1999) The SIR2/3/4 complex and SIR2 alone promote longevity in *Saccharomyces cerevisiae* by two different mechanisms. *Genes & Development* 13(19):2570-2580.
2. Hirsch BM & Zheng W (2011) Sirtuin mechanism and inhibition: explored with N(epsilon)-acetyl-lysine analogs. *Molecular bioSystems* 7(1):16-28.
3. Cen Y (2010) Sirtuins inhibitors: the approach to affinity and selectivity. *Biochimica et biophysica acta* 1804(8):1635-1644.
4. Sauve AA (2010) Sirtuin chemical mechanisms. *Biochimica Et Biophysica Acta-Proteins and Proteomics* 1804(8):1591-1603.
5. Hu P, Wang S, & Zhang Y (2008) Highly dissociative and concerted mechanism for the nicotinamide cleavage reaction in Sir2Tm enzyme suggested by ab initio QM/MM molecular dynamics simulations. *Journal of the American Chemical Society* 130(49):16721-16728.
6. Zhou Y, et al. (2012) The bicyclic intermediate structure provides insights into the desuccinylation mechanism of human sirtuin 5 (SIRT5). *The Journal of biological chemistry* 287(34):28307-28314.
7. Mercken EM, et al. (2014) SIRT2104 extends survival of male mice on a standard diet and preserves bone and muscle mass. *Aging Cell* 13(5):787-796.
8. Mitchell SJ, et al. (2014) The SIRT1 activator SIRT1720 extends lifespan and improves health of mice fed a standard diet. *Cell Rep* 6(5):836-843.
9. Zorn JA & Wells JA (2010) Turning enzymes ON with small molecules. *Nat Chem Biol* 6(3):179-188.
10. Sinclair DA & Guarente L (2014) Small-molecule allosteric activators of sirtuins. *Annual review of pharmacology and toxicology* 54:363-380.
11. Hubbard BP, et al. (2013) Evidence for a Common Mechanism of SIRT1 Regulation by Allosteric Activators. *Science* 339(6124):1216-1219.
12. Dai H, et al. (2015) Crystallographic structure of a small molecule SIRT1 activator-enzyme complex. *Nat Commun* 6:7645.
13. Lakshminarasimhan M, Rauh D, Schutkowski M, & Steegborn C (2013) Sirt1 activation by resveratrol is substrate sequence-selective. *Aging (Albany NY)* 5(3):151-154.
14. North BJ, et al. (2014) SIRT2 induces the checkpoint kinase BubR1 to increase lifespan. *Embo Journal* 33(13):1438-1453.
15. Brown K, et al. (2013) SIRT3 reverses aging-associated degeneration. *Cell Rep* 3(2):319-327.
16. Kanfi Y, et al. (2012) The sirtuin SIRT6 regulates lifespan in male mice. *Nature* 483(7388):218-221
17. Moniot S, et al (2012) Structures, Substrates, and Regulators of Mammalian Sirtuins – Opportunities and Challenges for Drug Development *Frontiers in Pharmacology*. 2012; 3: 16
18. Gertz M, et al. (2013) Ex-527 inhibits Sirtuins by exploiting their unique NAD(+) -dependent deacetylation mechanism. *Proceedings of the National Academy of Sciences of the United States of America* 110(30):E2772-E2781.
19. Rumpf T, et al. (2015) Selective Sirt2 inhibition by ligand-induced rearrangement of the active site. *Nat Commun* 6:6263.
20. Gomes AP, et al. (2013) Declining NAD(+) induces a pseudohypoxic state disrupting nuclear-mitochondrial communication during aging. *Cell* 155(7):1624-1638.
21. Qin WP, et al. (2006) Neuronal SIRT1 activation as a novel mechanism underlying the prevention of Alzheimer disease amyloid neuropathology by calorie restriction. *Journal of Biological Chemistry* 281(31):21745-21754.
22. Satoh A & Imai S (2014) Systemic regulation of mammalian ageing and longevity by brain sirtuins. *Nat Commun* 5:4211.
23. Massudi H, et al. (2012) Age-Associated Changes In Oxidative Stress and NAD(+) Metabolism In Human Tissue. *Plos One* 7(7):e42357.
24. Canto C, et al. (2012) The NAD(+) precursor nicotinamide riboside enhances oxidative metabolism and protects against high-fat diet-induced obesity. *Cell Metab* 15(6):838-847.
25. Smith BC & Denu JM (2007) Sir2 deacetylases exhibit nucleophilic participation of acetyl-lysine in NAD⁺ cleavage. *Journal of the American Chemical Society* 129(18):5802-5803.
26. Avalos JL, Boeke JD, & Wolberger C (2004) Structural basis for the mechanism and regulation of Sir2 enzymes. *Molecular Cell* 13(5):639-648.
27. Liang Z, et al. (2010) Investigation of the catalytic mechanism of Sir2 enzyme with QM/MM approach: SN1 vs SN2? *The journal of physical chemistry. B* 114(36):11927-11933.
28. Shi YW, Zhou YZ, Wang SL, & Zhang YK (2013) Sirtuin Deacetylation Mechanism and Catalytic Role of the Dynamic Cofactor Binding Loop. *J. Phys. Chem. Lett.* 4(3):491-495.
29. Avalos JL, Bever KM, & Wolberger C (2005) Mechanism of sirtuin inhibition by nicotinamide: Altering the NAD(+) cosubstrate specificity of a Sir2 enzyme. *Molecular Cell* 17(6):855-868.
30. Guan X, Lin P, Knoll E, & Chakrabarti R (2014) Mechanism of inhibition of the human sirtuin enzyme SIRT3 by nicotinamide: computational and experimental studies. *PLoS One* 9(9):e107729.
31. Cen Y & Sauve AA (2010) Transition state of ADP-ribosylation of acetyllysine catalyzed by *Archaeoglobus fulgidus* Sir2 determined by kinetic isotope effects and computational approaches. *Journal of the American Chemical Society* 132(35):12286-12298.
32. Sauve AA, Moir RD, Schramm VL, & Willis IM (2005) Chemical activation of Sir2-dependent silencing by relief of nicotinamide inhibition. *Molecular Cell* 17(4):595-601.
33. Hawse WF, et al. (2008) Structural Insights Into Intermediate Steps in the Sir2 Deacetylation Reaction. *Structure* 16(9):1368-1377.
34. Jin L, et al. (2009) Crystal Structures of Human SIRT3 Displaying Substrate-induced Conformational Changes. *The Journal of Biological Chemistry*. 284(36): 24394-24405.
35. Armstrong CM, Kaeberlein M, Imai SI, & Guarente L (2002) Mutations in *Saccharomyces cerevisiae* gene SIR2 can have differential effects on in vivo silencing phenotypes and in vitro histone deacetylation activity. *Mol Biol Cell* 13(4):1427-1438.
36. Szczepankiewicz BG, et al. (2012) Synthesis of carba-NAD and the structures of its ternary complexes with SIRT3 and SIRT5. *The Journal of organic chemistry* 77(17):7319-7329.
37. Zhao KH, Harshaw R, Chai XM, & Marmorstein R (2004) Structural basis for nicotinamide cleavage and ADP-ribose transfer by NAD(+) -dependent Sir2 histone/protein deacetylases. *Proceedings of the National Academy of Sciences of the United States of America* 101(23):8563-8568.
38. Sauve AA & Schramm VL (2003) Sir2 regulation by nicotinamide results from switching between base exchange and deacetylation chemistry. *Biochemistry* 42(31):9249-9256.
39. Hockerman GH, Peterson BZ, Johnson BD, & Catterall WA (1997) Molecular determinants of drug binding and action on L-type calcium channels. *Annual review of pharmacology and toxicology* 37:361-396.
40. Mai A, et al. (2009) Study of 1,4-dihydropyridine structural scaffold: discovery of novel sirtuin activators and inhibitors. *J Med Chem* 52(17):5496-5504.
41. Jackson MD, Schmidt MT, Oppenheimer NJ, & Denu JM (2003) Mechanism of nicotinamide inhibition and transglycosylation by Sir2 histone/protein deacetylases. *The Journal of biological chemistry* 278(51):50985-50998.
42. Sauve AA & Schramm VL (2003) Nicotinamide inhibition of SIR2 is a consequence of chemical competition for an ADPR - peptidyl intermediate. *Biochemistry* 42(28):8630-8630.
43. Imai S (2010) A possibility of nutraceuticals as an anti-aging intervention: Activation of sirtuins by promoting mammalian NAD biosynthesis. *Pharmacological research : the official journal of the Italian Pharmacological Society* 62(1):42-47.
44. Pacholec M, et al. (2010) SIRT1720, SIRT2183, SIRT1460, and Resveratrol Are Not Direct Activators of SIRT1. *Journal of Biological Chemistry* 285(11):8340-8351.
45. Wang G, et al. (2014) P7C3 neuroprotective chemicals function by activating the rate-limiting enzyme in NAD salvage. *Cell* 158(6):1324-1334.
46. Hawse WF & Wolberger C (2009) Structure-based Mechanism of ADP-ribosylation by Sirtuins. *Journal of Biological Chemistry* 284(48):33654-33661.
47. Chakrabarti R, Klibanov AM, Friesner RA (2005) Sequence optimization and designability of enzyme active sites. *Proceedings of the National Academy of Sciences of the United States of America* 102: 12035-12040.

Please review all the figures in this paginated PDF and check if the figure size is appropriate to allow reading of the text in the figure.

If readability needs to be improved then resize the figure again in 'Figure sizing' interface of Article Sizing Tool.